Syst. Biol. 71(5):1032–1044, 2022

DOI:10.1093/sysbio/syac001
Advance Access publication January 18, 2022

Phylogenomics of Bony-Tongue Fishes (Osteoglossomorpha) Shed Light on the Craniofacial Evolution and Biogeography of the Weakly Electric Clade (Mormyridae)

ROSE D. PETERSON[1,*], JOHN P. SULLIVAN[2], CARL D. HOPKINS[2,3], AINTZANE SANTAQUITERIA[4], CASEY B. DILLMAN[2,5], STACY PIRRO[6], RICARDO BETANCUR-R[4], DAHIANA ARCILA[4,7], LILY C. HUGHES[8], AND GUILLERMO ORTÍ[1,9]

[1]*Department of Biological Sciences, The George Washington University, Bell Hall 2029 G Street NW Suite 302, Washington, DC 20052, USA;* [2]*Cornell University Museum of Vertebrates, Ithaca, NY, USA;* [3]*Department of Neurobiology and Behavior, Cornell University, Ithaca, NY, USA;* [4]*Department of Biology, University of Oklahoma, Norman, OK, USA;* [5]*Department of Ecology and Evolutionary Biology, Cornell University, Ithaca, NY, USA;* [6]*Iridian Genomes Inc., Bethesda, MD, USA;* [7]*Department of Ichthyology, Sam Noble Oklahoma Museum of Natural History, Norman, OK, USA;* [8]*Department of Organismal Biology and Anatomy, University of Chicago, Chicago, IL, USA; and* [9]*Department of Vertebrate Zoology, National Museum of Natural History, Smithsonian Institution, Washington, DC, USA*

[*]*Correspondence to be sent to: Department of Biological Sciences, The George Washington University, Bell Hall 2029 G Street NW Suite 302, Washington, DC 20052, USA; E-mail: rosepeterson@gwu.edu.*

Received 23 May 2021; reviews returned 3 January 2022; accepted 10 January 2022
Associate Editor: Rachel Mueller

Abstract.—Bonytongues (Osteoglossomorpha) constitute an ancient clade of teleost fishes distributed in freshwater habitats throughout the world. The group includes well-known species such as arowanas, featherbacks, pirarucus, and the weakly electric fishes in the family Mormyridae. Their disjunct distribution, extreme morphologies, and electrolocating capabilities (Gymnarchidae and Mormyridae) have attracted much scientific interest, but a comprehensive phylogenetic framework for comparative analysis is missing, especially for the species-rich family Mormyridae. Of particular interest are disparate craniofacial morphologies among mormyrids which might constitute an exceptional model system to study convergent evolution. We present a phylogenomic analysis based on 546 exons of 179 species (out of 260), 28 out of 29 genera, and all six families of extant bonytongues. Based on a recent reassessment of the fossil record of osteoglossomorphs, we inferred dates of divergence among transcontinental clades and the major groups. The estimated ages of divergence among extant taxa (e.g., Osteoglossomorpha, Osteoglossiformes, and Mormyroidea) are older than previous reports, but most of the divergence dates obtained for clades on separate continents are too young to be explained by simple vicariance hypotheses. Biogeographic analysis of mormyrids indicates that their high species diversity in the Congo Basin is a consequence of range reductions of previously widespread ancestors and that the highest diversity of craniofacial morphologies among mormyrids originated in this basin. Special emphasis on a taxon-rich representation for mormyrids revealed pervasive misalignment between our phylogenomic results and mormyrid taxonomy due to repeated instances of convergence for extreme craniofacial morphologies. Estimation of ancestral phenotypes revealed contingent evolution of snout elongation and unique projections from the lower jaw to form the distinctive Schnauzenorgan. Synthesis of comparative analyses suggests that the remarkable craniofacial morphologies of mormyrids evolved convergently due to niche partitioning, likely enabled by interactions between their exclusive morphological and electrosensory adaptations. [Africa; ancestral state estimation; diversity; exon capture; freshwater fishes; Phylogenomics.]

Convergent evolution of phenotypic traits has been documented in many branches of the tree of life, raising fundamental questions about the relative importance of chance and selective forces on the process of evolution (Gould 1989; Losos 1998). These questions can be addressed at different levels of organization (e.g., genetic, physiological, developmental, and anatomical) and at vastly different time frames, ranging from microevolution among closely related species or populations of the same species (e.g., Rundle et al. 2000; Hoekstra et al. 2006) to large scale macroevolutionary convergence among distantly related lineages (McGhee 2001). These comparisons, however, can only be framed in reference to a phylogeny that includes repeated evolution of the "same" trait along separate lineages (Felsenstein 1985).

The focus of this study is an early-branching clade of freshwater fishes with about 260 living species, classified in the super-cohort Osteoglossomorpha (the "bonytongues"), in which we document repeated instances of morphological convergence. This group includes charismatic arowanas and arapaimas (Osteoglossidae), featherbacks (Notopteridae), elephant-nose fishes (Mormyridae), and African butterflyfishes (Pantodontidae), among others. The pan-African family Mormyridae is by far the most species-rich (232 species) and morphologically diverse clade within Osteoglossomorpha, but their phylogeny is poorly known. Their diversity and geographic restriction to the African continent, with the highest species diversity found in the Congo Basin, make Mormyridae a good candidate for fine-scale biogeographic and morphological analyses. The only other clade of freshwater electric fishes of comparable diversity and continent-wide distribution are the distantly related South American knifefishes (Gymnotiformes). These two groups share many convergent phenotypic and ecological traits—namely, nocturnal lifestyles enabled by electrolocation for navigation, food acquisition, defense, and communication, and distinctive craniofacial morphologies (Lavoué et al. 2012). But rampant convergence also seems to be present within each clade.

While studies of mormyrids focused on the evolution and physiology of electric organs and behavior associated with electroreception (e.g., Lissmann 1958; Hopkins and Bass 1981; Caputi et al. 2005; Gallant et al. 2014), less attention has been devoted to their remarkable variation in craniofacial morphologies (CFMs) associated with their mouth and jaws (Fig. 1), which are densely covered with electroreceptors (Bacelo et al. 2008; Hollmann et al. 2008; Amey-Özel et al. 2012). Some extreme CFMs in the genera *Mormyrus* and *Mormyrops* include "tubesnouts," with a bony elongations of their head with small pincer-like jaws at the anterior end (Fig. 1j). The tubesnout phenotype is not uncommon in other teleost lineages (e.g., armored sticklebacks, spikefishes, pipefishes, and seahorses), suggesting that this morphology convergently evolved in fishes as a feeding specialization across deep time. However, only mormyrids and gymnotiforms have independently acquired tubesnouts that are densely covered with electroreceptors (Castelló et al. 2000; Sullivan et al. 2000; Albert 2001; Evans et al. 2017). The remarkable convergence of tubesnout morphology and function in weakly electric gymnotiforms and mormyrids seems to have evolved in concert with their unique electrosensory systems, allowing them to exploit novel trophic niches, such as extracting prey from crevices with a "grasp-suction" method (Marrero and Winemiller 1993; Lavoué et al. 2012). Other unique CFMs of mormyrids associated with foraging behavior include a "chin-swelling"—a fleshy mass protruding from the lower jaw—as seen in *Marcusenius* (Fig. 1l), and the Schnauzenorgan—a fingerlike appendage projecting from the lower jaw—that is typical of the genus *Gnathonemus* (Fig. 1k; Stendall 1916). Some species, such as *Campylomormyrus mirus*, have the most extreme CFM that combines both a tubesnout and a Schnauzenorgan (Fig. 1m). Most mormyrids, however, are not characterized by any CFM protrusion and are referred to here as "blunt-nose" phenotypes. An early phylogenetic study of mormyrids (Sullivan et al. 2000) suggested that the chin-swelling, tubesnout, and Schnauzenorgan CFMs might have evolved independently in several genera, muddling their utility as diagnostic characters for taxonomy. But previous phylogenetic studies of mormyrids have analyzed relatively few taxa because many species occur in remote, hard-to-sample locations, and therefore are rare in museum collections (Sullivan et al. 2000, 2002; Lavoué et al. 2000).

The oldest osteoglossomorph fossils date back to the Early Jurassic (206.9–167 Ma, Capobianco and Friedman (2019), but molecular phylogenies push their origin as far back as 260–197 Ma (Broughton et al. 2013). Fossil osteoglossomorphs are found in every continent besides Antarctica (Greenwood et al. 1966; Hilton 2003), and extant taxa are only absent from Europe. Their disjunct global distribution in freshwater habitats prompted contrasting biogeographic hypotheses such as vicariance due to Gondwana break-up and transoceanic dispersal (e.g., Nelson 1969; Lundberg 1993; Inoue et al. 2009; Hilton and Forey 2015; Lavoué 2016). But phylogenetic relationships among osteoglossomorphs (Fig. 1a–d) have been contentious mainly due to the unstable position of the enigmatic African butterflyfish *Pantodon buchholzi* (Fig. 1f) and poor taxon sampling among mormyrids, hampering comparative studies (Li and Wilson 1996; Hilton 2003; Lavoué and Sullivan 2004; Zhang 2006; Bonde 2008; Lavoué 2016; Hilton and Lavoué 2018; Murray et al. 2018). Mormyrids have a fragmentary fossil record restricted to Africa (Greenwood 1972; Hilton 2003; Lavoué and Sullivan 2004; Wilson and Murray 2008; Lavoué et al. 2012; Lavoué 2016; Hilton and Lavoué 2018) and extant species have a Pan-African distribution, occurring in seven of nine ichthyofaunal provinces, with highest diversity in the Congo Basin (Lévêque et al. 2008). This pattern, also reported for other African freshwater fishes, is consistent with a hypothesis considering the Congo Basin as a source of diversity for more depauperate areas (Livingstone et al. 1982). Palaeohydrological and paleoclimatic changes also have been suggested to promote diversification of African freshwater organisms (Lundberg 1998; Montoya-Burgos 2003), especially increasing temperatures and precipitation during the Middle Miocene (Flower and Kennett 1994; Zachos et al. 2001) that may have increased connections between river basins. Africa has a rich ichthyofaunal diversity, but the patterns and processes responsible for this diversity are poorly understood (Lévêque and Paugy 2017; Arroyave et al. 2020).

Here, we develop a phylogenomic framework based on 546 exon sequences and a taxonomically dense sampling of ostoglossomorphs, with the most complete representation of mormyrids to date. Integrating neontological and paleontological data, we reassess the timing of diversification of osteoglossomorphs and test macroevolutionary processes involving African mormyrids, including their biogeography and the evolution of CFMs. By combining a dense taxon sampling and genome-wide markers, our results provide new insights into the diversification of this iconic clade of early-diverging teleosts and reveal several instances of convergent evolution of their unique morphological innovations.

Materials and Methods

Taxon Sampling

A total of 197 specimens were included in the molecular analysis presented in this study (Table S1 of the Supplementary material available on Dryad at http://dx.doi.org/10.5061/dryad.31zcrjdkm), counting 10 individuals that have publicly accessible data (Lamanna et al. 2015; Gallant et al. 2017; Estefano et al. 2018; Hughes et al. 2018). Taxonomic sampling for the ingroup (Osteoglossomorpha; Arratia 1999) included 187 individuals representing 179 species out of ~260,

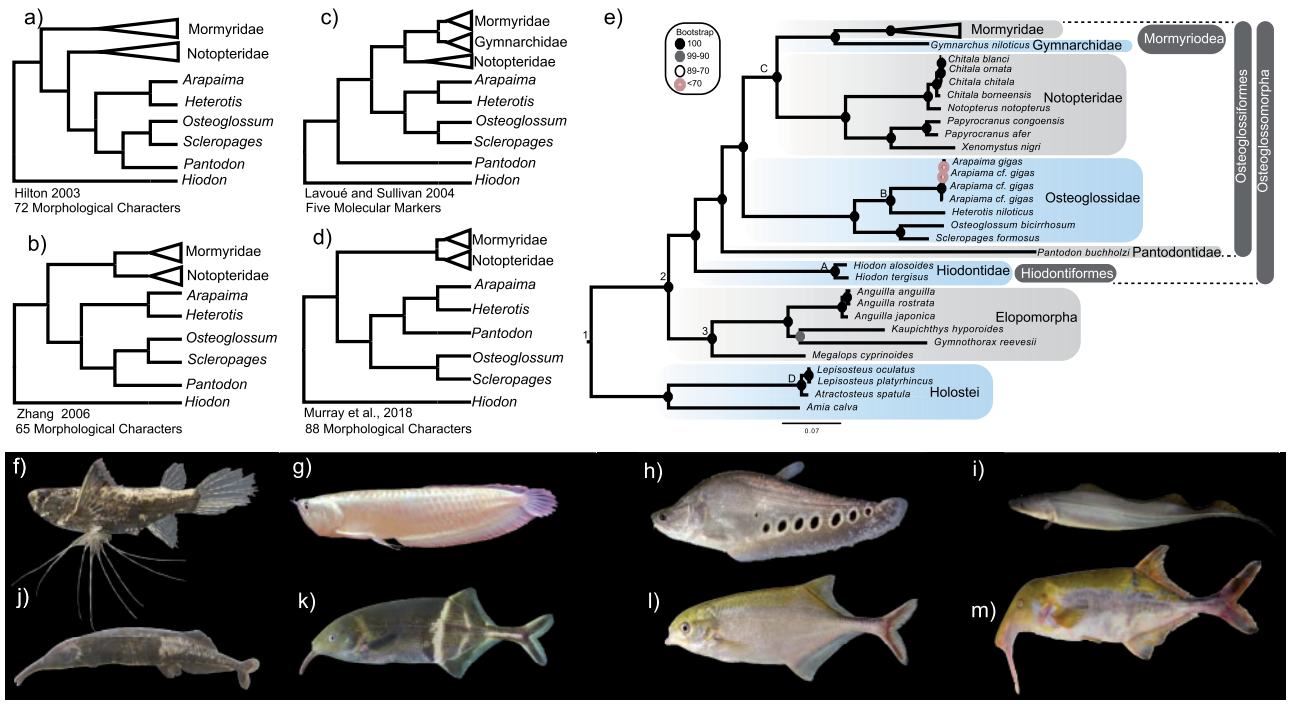

FIGURE 1. a–d) previous morphological and molecular phylogenetic hypotheses for Osteoglossomorpha. Intercontinental sister-group relationships implied by these phylogenies include (i) *Arapaima* (South America) and *Heterotis* (Africa), (ii) *Scleropages* (Australia and Southeast Asia) and *Osteoglossum* (South America), and (iii) Asian and African Notopterids (relationships not shown). e) Maximum likelihood tree for Osteoglossomorpha based on a concatenated 546 exon data set (this study). Numbers (1–3) identify nodes that were constrained with secondary calibrations and letters (A–D) nodes constrained by fossils for the time-tree analysis. Photographs represent morphological diversity among osteoglossomorphs and cranialfacial morphology in Mormyridae. f) *Pantodon buchholzi* (Pantodontidae); g) *Osteoglossum bicirrhosum* (Osteoglossidae); h) *Chitala chitala* (Notopteridae; UF fish 237959); i) *Gymnarchus niloticus* (Gymnarchidae); j) *Mormyrops boulengeri* (tubesnout; CUMV 97526); k) *Gnathonemus petersii* (Schnauzenorgan; CUMV 96749); l) *Marcusenius stanleyanus* (chin swelling; CUMV 96481); and m) *Campylomormyrus mirus* (tube snout with Schnauzenorgan; CUMV 9705). Photo credits: John P. Sullivan (f, j–m), Xomenka licensed under CC BY 3.0 (g), Zachary Randall, Florida Museum of Natural History (h), Ellicrum licensed under CC BY-SA 3.0 (i).

and all six families. The only genus not sampled was *Heteromormyrus* (Mormyridae), only known from the holotype (Steindachner 1866). The outgroup sampling included 10 species from Elopomorpha and Holostei. Voucher information is listed in Table S1 of the Supplementary material available on Dryad.

DNA Extraction and Sequencing

We extracted genomic DNA from muscle or fin clips at the Laboratory of Analytical Biology, Smithsonian Institution National Museum of Natural History. Extractions followed the standard animal tissue phenol protocol for the Gene Prep (Autogen) platform. We used the "Backbone 1" probe set to enrich libraries for a set of 1105 target exons defined by Hughes et al. (2021). Library preparation and exon capture were performed by Arbor Biosciences (Ann Arbor, MI) on 153 samples. Enriched libraries were pooled and sequenced at the University of Chicago Genomic facility on a HiSeq 4000 lane with paired-end 100 bp reads. Whole-genome sequencing (WGS) was performed on 44 individuals for an upcoming project on comparative genomics (WGS; Table S1 of the Supplementary material available on Dryad). Tissue samples for these taxa were shipped to GeneWiz (South Plainfield, New Jersey) for DNA extraction, library preparation, and sequencing. These libraries were "shotgun" sequenced on an Illumina HiSeq X Ten multiplexing five samples per lane to obtain 150 bp paired-end reads (more details in Supplementary Methods available on Dryad).

Quality Control, Sequence Assembly, and Alignments

The assembly of exon sequences from raw-reads obtained by the exon-capture protocol followed the bioinformatics pipeline described by Hughes et al. (2021). For the 44 taxa with WGS data, we filtered low quality and short reads using Trimmomatic v0.39 (Bolger et al. 2014) and assembled trimmed reads into scaffolds with SOAPdenovo2 v2.04-r240 (Luo et al. 2015). The 1105 targeted exons were extracted from these scaffolds using HMMER v3.1b (Wheeler and Eddy 2013) following Hughes et al. (2018). Sequences were aligned with MACSE v2.03 (Ranwez et al. 2018). To minimize missing data, we excluded exon alignments with <50% of taxa present from any downstream analysis. We visually inspected gene trees where Mormyridae was not monophyletic to minimize the potential effect of

paralogous sequences and potential cases of cross-contamination. Misplaced taxa or the complete exon alignment were excluded from downstream analysis after visual inspection. Finally, we used TreeShrink (Mai and Mirarab 2018), a quality control utility designed to identify and remove misplaced taxa in gene trees. Additional quality control steps implemented are explained in Supplementary Methods available on Dryad.

Phylogenomic Inference

We concatenated exon alignments that passed quality control filters into a single alignment and partitioned the entire matrix into three subsets according to codon position. We used the "TESTMERGE" option of ModelFinder (Kalyaanamoorthy et al. 2017) in IQ-TREE v1.6.11 (Nguyen et al. 2015) to find the best-fitting substitution model for merged partitions. IQ-TREE was also used to estimate a concatenation-based phylogeny under maximum likelihood (ML) using 10 independent runs, with node support assessed by 1000 ultrafast bootstrap replicates (Hoang et al. 2018). Individual gene-trees were estimated using IQ-TREE, with the same search parameters. To minimize the negative impact of gene-tree estimation error when using two-step multispecies-coalescent methods (Simmons and Gatesy 2021), gene-tree branches with <50% bootstrap support were collapsed using TreeCollapseCL v4 (Hodcroft 2012), and used as input for ASTRAL-III (Zhang et al. 2017). Local posterior probability support values (Sayyari and Mirarab 2016) were calculated for ASTRAL trees. Finally, to account for phylogenetic uncertainty in downstream comparative analyses, we created 10 data subsets consisting of 50–60 genes each (following Rincon-Sandoval et al. 2020; Santaquiteria et al. 2021). This number of subsets is a tradeoff between obtaining enough replicates (10) while keeping sufficient data (exons) within each subset (50–60 exons). Although more replicates (>10) would have been desirable, a lower number of exons per subset would have diminished the quality of the inference and inflated gene-tree uncertainty beyond reasonable limits (more details in Supplementary Methods available on Dryad). A ML analysis with IQ-TREE and a two-step coalescent analysis with ASTRAL-III were run for each subset, as above. We visualized topological discordance among phylogenies by plotting all our trees (total data set and 10 subsets; 22 topologies total) using multidimensional scaling implemented in the R package *phytools* (Revell 2012). The topology obtained with IQ-TREE on the concatenated full data matrix was used as a reference (henceforth the "master" tree).

Divergence-time Estimation

All 22 topologies were time-calibrated using four fossil taxa and three secondary calibrations (Fig. 1e, Supplementary Methods available on Dryad and Table S3 of the Supplementary material available on Dryad). Based on a recent review of the paleontological record of osteoglossiforms (Hilton and Lavoué 2018), we included †*Atractosteus falipoui* (crown Lepisosteidae; Benton et al. 2015), †*Hiodon woodruffi* (crown *Hiodon;* Hilton and Grande 2008), †*Sinoglossus lushanensis* (trichotomy with *Heterotis* and *Arapaima;* Li and Wilson 1996; Lavoué 2016), and †*Palaeonotopterus greenwoodi* (stem mormyroid Hilton 2003; Wilson and Murray 2008). These fossils were assigned to specific nodes (present in all 22 topologies, Fig. 1e) based on the classification provided in the most current literature. We used a uniform distribution as a prior to constrain these nodes by enforcing a hard-minimum age based on the youngest age interpretation of the fossil and a soft maximum age. This prior ensures that the calibrated node is at least as old as the estimated age of the corresponding fossil and allows for uncertainty in maximum age due to incompleteness and sampling biases in the fossil record. Secondary calibrations obtained from prior studies by Betancur et al. (2013), Hughes et al. (2018), Broughton et al. (2013), and Giles et al. (2017) were applied to specific nodes to enforce soft maximum age and hard minimum age priors using a uniform distribution (Fig. 1e; Table S3 of the Supplementary material available on Dryad). We implemented these priors in the program MCMCTree (PAMLv4.9; Yang 2007), an approximate likelihood approach in a Bayesian Framework (dos Reis and Yang 2019), that is less computationally expensive than other full-likelihood approaches and, therefore, more suitable for genome-scale data sets. To assess the uncertainty that may arise by sampling molecular data, we also estimated divergence times for trees inferred from the ten nonoverlapping subsets of exons. The all-genes ASTRAL tree did not converge and was excluded from downstream analyses (ESS values <200). More details are available in Supplementary Methods available on Dryad.

Craniofacial Morphology Evolution in Mormyridae

Evolutionary analysis of CFM was based on the estimation of transition rates among discrete phenotypes characterized for mormyrid taxa (Fig. 1). We assigned each terminal taxon to one of five CFM states (Appendix 3 of the Supplementary material available on Dryad): (0) blunt-nose, (1) chin-swelling, (2) tubesnout, (3) Schnauzenorgan, (4) tubesnout with Schnauzenorgan. We implemented stochastic character mapping (Bollback 2006) to estimate ancestral states and transition rates along the phylogeny with the *make.simmap* function available in the R package *phytools* (Revell 2012). The time-calibrated tree topology inferred with IQ-TREE using all genes was used as the reference phylogeny. We chose the best-fitting model according to AICc values among the following options: Equal Rates, Symmetric Rates (SYM), or All Rates Different. To account for phylogenetic uncertainty, we ran 100 simulations for each of the 21 time-trees estimated (see above) after pruning taxa to include only Mormyridae. Transition rates among states were averaged across all simulations.

For example, if the 1-to-2 character-state transformation was estimated to occur in 14 instances across the 100 simulations (on average) for each tree, then the reported rate (or probability) for this transformation would be 0.14, interpreted to be close to zero and therefore receiving no support from this analysis.

Biogeographic Analyses of Mormyridae

African freshwater biogeographic regions proposed by Lévêque et al. (2008) and occupied by mormyrids include Upper Guinea (UG), Lower Guinea (LG), Nilo-Sudanic (NS), Zambezi (Z), East Coast (EC), Congo Basin (CB), and Quanza (Q). A species-by-region matrix (Table S6) was coded for presence or absence of extant mormyrid species using FishBase (Froese and Pauly 2000), FaunAfri (Paugy et al. 2008) and field observations by J.P. Sullivan. We estimated ancestral ranges using the R package BioGeoBEARS (Matzke 2013). Two different dispersal schemes were implemented to model evolution among biogeographic regions: (M0) assumes that dispersal between any pair of regions is equally likely, following Arroyave et al. (2020); (M1) assumes constraints to dispersal contingent on the proximity and connectivity between regions and the dispersal capability of extant species (basins that are next to each other are given 100% of probability for dispersal, while areas that are not connected have a probability of 0.01%). For each dispersal scheme, we evaluated 12 biogeographic models including "DEC" (Ree and Smith 2008), "DIVA" (Ronquist 1997), and "BayAREA" (Landis et al. 2013), with and without the *j* parameter (Matzke 2014), and with and without the *w* parameter (Dupin et al. 2017). Dispersal schemes and input files for BioGeoBEARS are listed in Supplementary Methods, Tables S6, S8, and Appendix 4 of the Supplementary material available on Dryad. To account for phylogenetic uncertainty, we implemented the best model on each of the 21 time-trees estimated (see above) after pruning taxa to include only Mormyridae (see Supplementary Methods available on Dryad for details).

Results

Phylogenetic Inference and Divergence Estimation for Osteoglossomorpha

Raw sequence data are available at NCBI Bioproject (PRJNA699339); for molecular data set properties and alignment files see Supplementary material (Appendix 1 of the Supplementary material available on Dryad). Most of the 22 phylogenies estimated from the complete 546 exon data set and exon subsets produced congruent and highly supported topologies resolving the major groupings within Osteoglossomorpha (Figs. 1–3, Figs. S1–S3 of the Supplementary material available on Dryad). Collectively, our results (Fig. 1e) support the hypothesis for family-level relationships of Osteoglossomorpha published by Lavoué and Sullivan (2004), and Betancur-R et al. (2017). A few exceptions in our subsets are noted in the Supplementary Results available on Dryad. However, given the overall concordant results, the topology inferred with IQ-TREE for the concatenated data set is used as our working hypothesis (the master tree) because trees inferred with ASTRAL for both the full data set and subsets contain many polytomies, particularly within Mormyridae (Fig. S3 of the Supplementary material available on Dryad).

The robust taxon sampling included in our phylogenetic analysis revealed a novel, rapidly evolving clade among mormyrids, that includes 51 morphologically diverse species in the genera *Campylomormyrus*, *Cyphomyrus*, *Gnathonemus*, *Genyomyrus*, *Hippopotamyrus*, and *Marcusenius* (Fig. 3; henceforth the "C+ clade"). Craniofacial morphologies present in this clade include the Schnauzenorgan, the tubesnout with Schnauzenorgan, and the chin-swelling phenotypes (Fig. 4), making this the most CFM-diverse clade among mormyrids. The rapid radiation of species and convergent evolution implied by our phylogeny (see below) likely misled previous taxonomic assignments, as shown by the nonmonophyly of three of the four C+ genera (Fig. 3): *Gnathonemus* (elephant fishes with Schnauzenorgan); *Marcusenius*, and *Hippopotamyrus* (both including species with chin swelling phenotypes, Figs. 2 and 3). These genera require taxonomic revision (Supplementary Results: Taxonomic Findings available on Dryad).

The time-calibrated phylogenies of the master tree and subsets are shown in Figure 4 and Figure S1 of the Supplementary material available on Dryad, respectively, and divergence-time estimates for select osteoglossomorph clades are shown in Table S5 of the Supplementary material available on Dryad. The origin of Osteoglossomorpha was estimated at 227.4 Ma (HPD 248.8–207 Ma) and Osteoglossiformes was inferred to have originated 197.7 Ma (HPD 221.6–174.4 Ma). The divergence of *Arapaima* (South American) and *Heterotis* (African) inferred to occur 45.4 Ma (HPD 48.2–41.6 Ma), while the estimated age for the divergence of *Scleropages* (SEA/Australian) and *Osteoglossum* (South American) was 38.2 Ma (HPD 50.9–24.9 Ma), but see Supplementary Materials available on Dryad for an alternative calibration using another fossil *Scleropages*. Asian (*Chitala* and *Notopterus*) and African (*Papyrocranus* and *Xenomystus*) notopterids diverged 69.29 Ma (HPD 78.7–60.3 Ma). Although the root of Mormyridae was estimated at 51.6 Ma (HPD 58.9–44.7 Ma), the explosive speciation with mormyrid Clade C+ is much more recent, starting only 13.1 Ma (HPD 15.1–11Ma) (Table S5 of the Supplementary material available on Dryad).

Ancestral State Estimation for Craniofacial Phenotypes

The SYM that assumes symmetric backward and forwards rates of transitions among CFMs was marginally the best fit for our data (Table S4 of the Supplementary material available on Dryad). The average number of changes among states, estimated

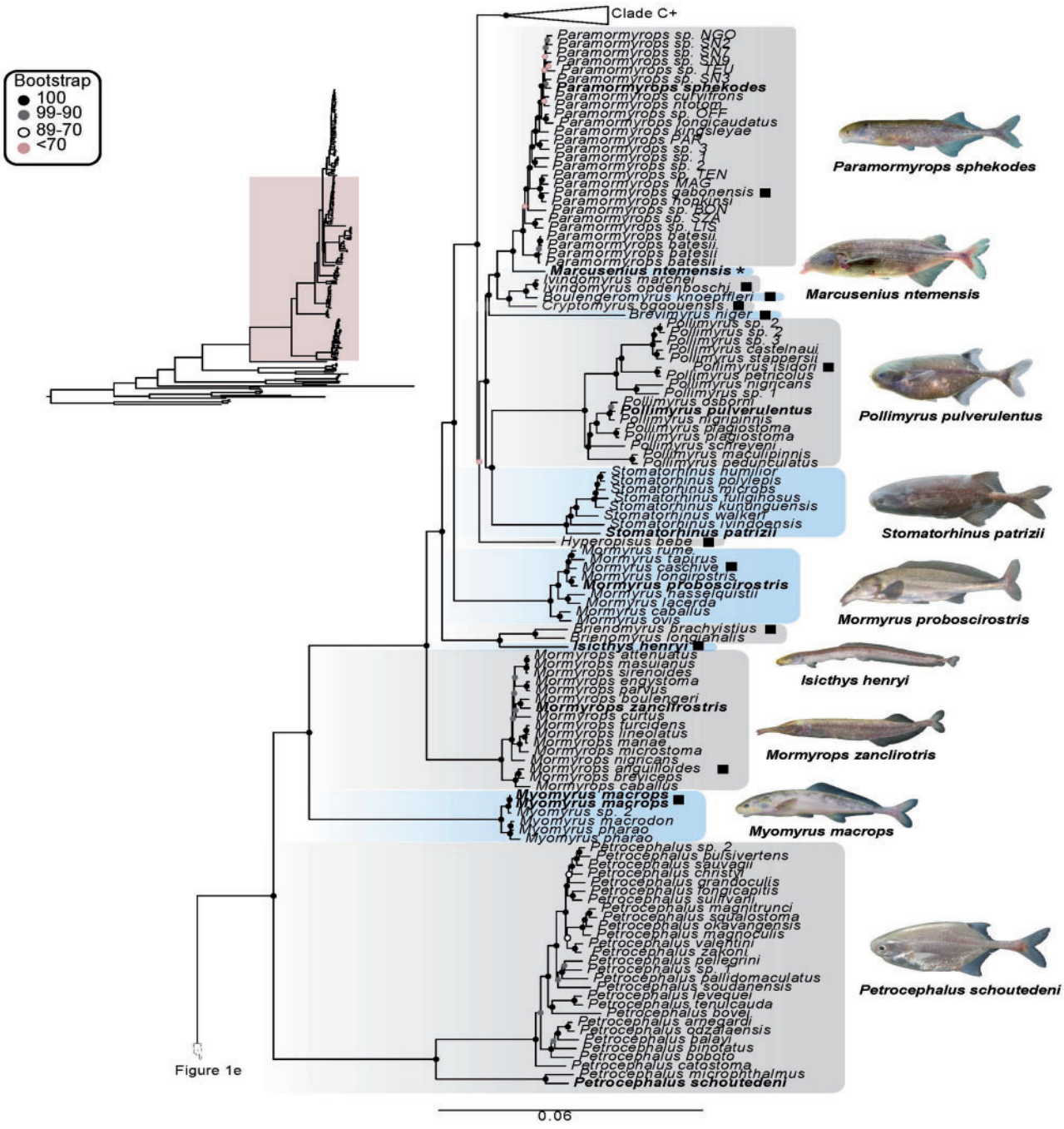

FIGURE 2. Maximum likelihood tree of Mormyridae based on the concatenated 546 exon matrix. The complete uncollapsed phylogeny is shown on the left with boxed area amplified here indicated by shading. Mormyridae Clade C+ (*Campylomormyrus*, *Gnathonemus*, *Hippopotamyrus*, and *Marcusenius*) is displayed in Figure 3. Taxa in need of revision (see Supplementary Results: Taxonomic Findings available on Dryad) are denoted by an asterisk and type species for a genus are marked with a black square. Scale bar units = substitutions/site. Photo credits: John P. Sullivan.

from 100 stimulations ran on the 21 time-calibrated topologies, indicates multiple transitions among CFM states. The most frequent transition among CFMs was from a blunt-nose to the chin-swelling state, estimated to occur six times among mormyrids (Fig. 4b). The second most frequent transition was from blunt-nose to tubesnout (four times). The origin of the Schnauzenorgan seems to be more complex due to its inferred association with the tubesnout state. In fact, the most frequent scenario obtained in our simulations estimates three independent transitions from chin-swelling directly to a tubesnout with Schnauzenorgan, and one transition from this state to the Schnauzenorgan (i.e., due to loss of the tubesnout phenotype). The transition from tubesnout to tubesnout with Schnauzenorgan was not obtained in any

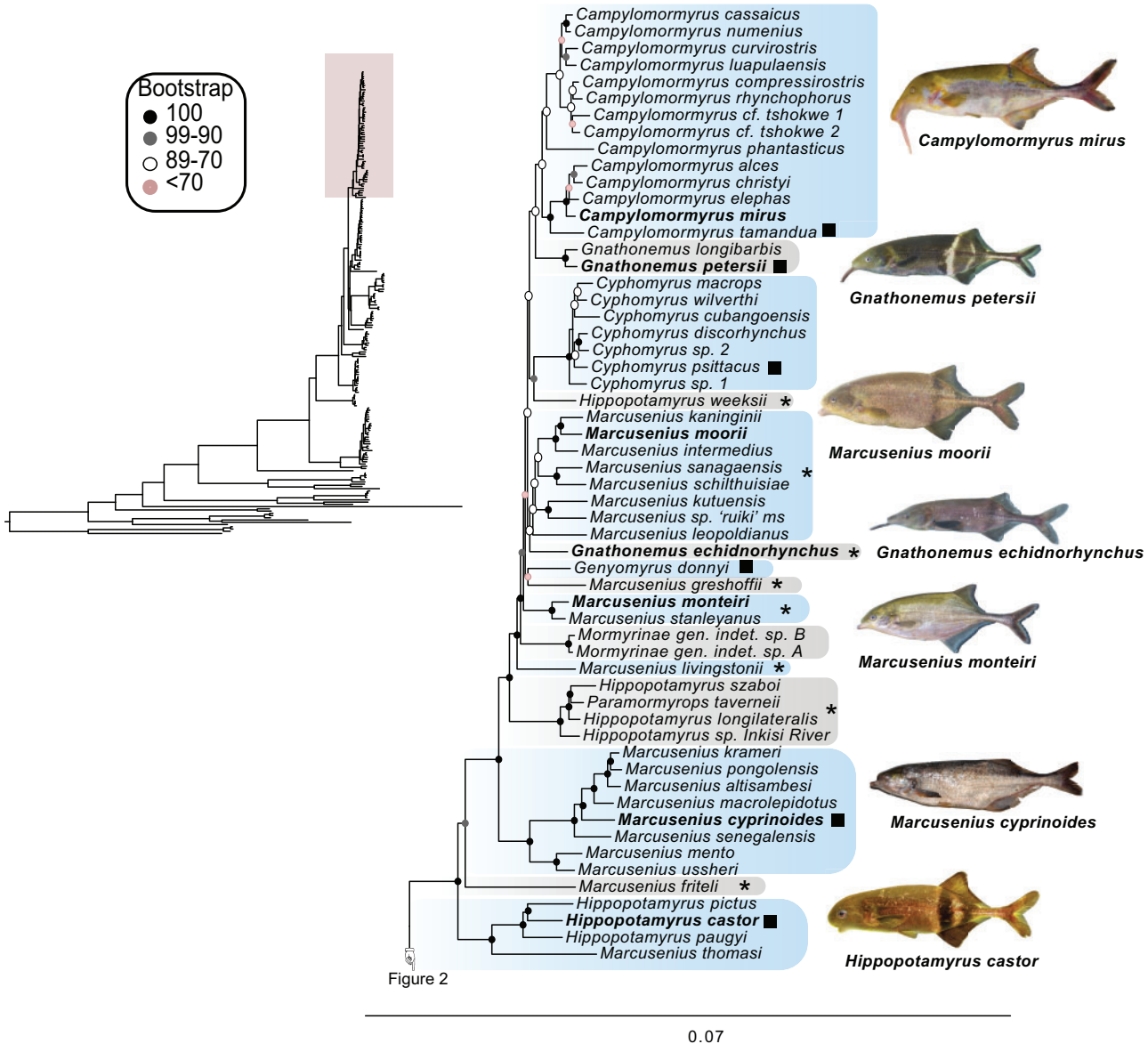

FIGURE 3. Maximum likelihood tree of Mormyridae Clade C+ based on the concatenated 546 exon matrix. The complete uncollapsed phylogeny is shown on the left with boxed area amplified here indicated by shading. Earlier diverging mormyrids are displayed in Figure 2. Taxa in need of revision (see Supplementary Results: Taxonomic Findings available on Dryad) are denoted by an asterisk and type species for a genus are marked with a black square. Scale bar units = substitutions/site. Photo credits: John P. Sullivan.

simulation. Likewise, the origin of the Schnauzenorgan directly from the chin-swelling state received very little support in this analysis ($P = 0.14$, Fig. 4b).

Biogeographic Analyses of Mormyridae in Africa

The majority of mormyrid taxa (58% of our sampled taxa) are present in the Congo Basin and 78% of these are endemic to this region. Outside of this basin, the Nilo-Sudanic region harbors the second-highest number of mormyrid species (17% of our sampled taxa) and 44% of them are endemics. In contrast, the Quanza region on the Atlantic coast of Africa has only one sampled species (*Hippopotamyrus* sp. Inkisi River). Mormyrid species from all biogeographic regions are distributed across the phylogeny, with all regions represented among the early branching as well as the most recently derived clades (Fig. 4a). But the C+ clade and *Mormyrops* seemed to have diversified primarily in the Congo Basin. The sister taxon to mormyrids is *Gymnarchus*, only present in the Nilo-Sudanic region.

Biogeographic models based on the M1 matrix assuming that dispersal capabilities of species are constrained by connectivity between regions were preferred over the unconstrained model (M0). The overall best likelihood and AICc score was obtained for

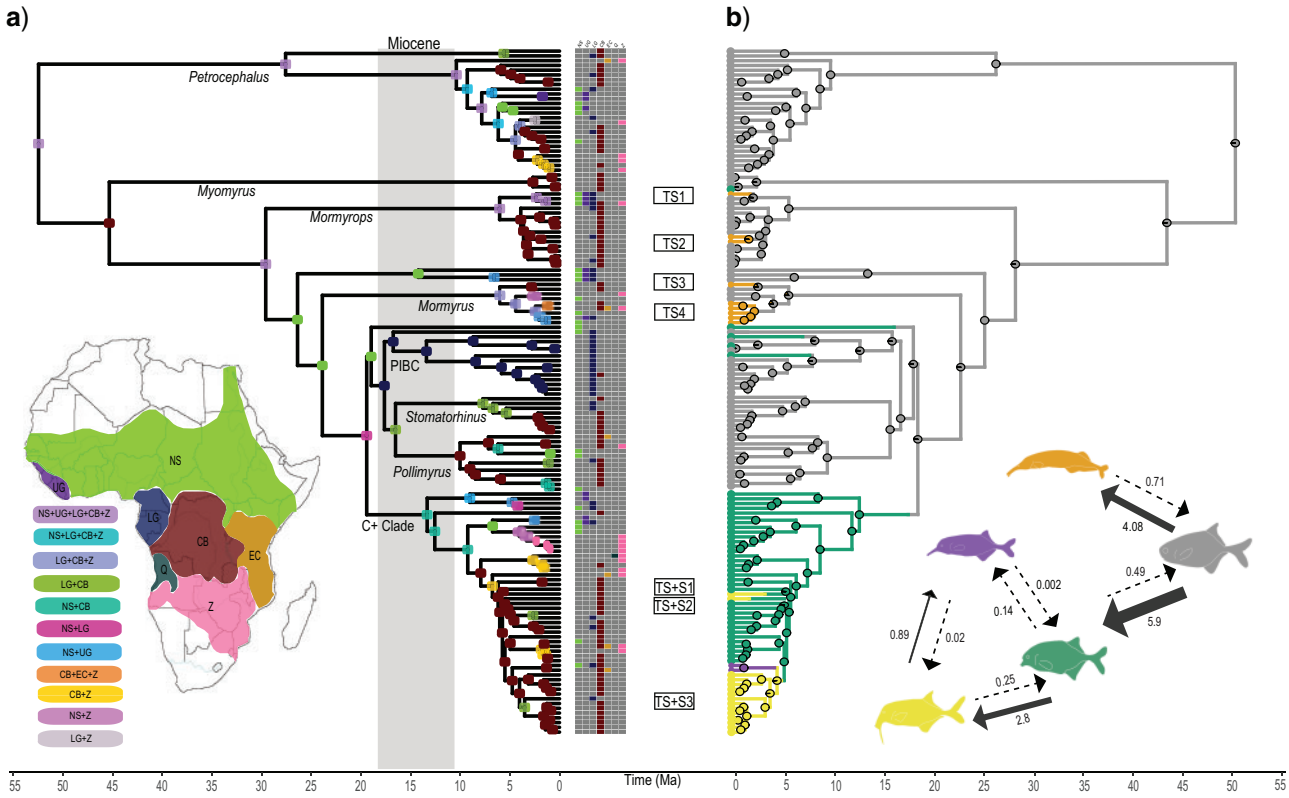

FIGURE 4. a) Biogeographic analysis of Mormyridae based on a time-calibrated phylogeny using BioGeoBEARS with the M1-DEC+w model (topology shown in detail in Figs. 2 and 3). Geographic areas considered are NS = Nilo-Sudanic; UG = Upper Guinea; LG = Lower Guinea; Q = Quanza; CB = Congo Basin; EC = East Coast; Z = Zambezi. Ancestral range estimations are shown with colored squares at the nodes. Boxes to the right of the phylogeny indicate the current range of extant species. b) Ancestral state estimation for CFMs in Mormyridae based on SIMMAP analyses using the same time-tree. Discrete phenotypes are indicated by different colors: blunt-nose (gray), chin swelling (green), tube snout (orange), Schnauzenorgan (purple), and tube snout with Schnauzenorgan (yellow). Pie charts at nodes represent the likelihoods of inferred ancestral states and circles at the tips represent each taxon's observed state. Arrows and fish figures on the lower-right show the average number of inferred character state transitions among phenotypes (averaged across 100-simulations run for each of 21 time-trees, under the SYM model. Text boxes between phylogenies denote inferred transitions to the tube snout (TS) or tube snout with Schnauzenorgan (TS+S) phenotypes that map to the Congo Basin (brown squares in a).

M1-DEC+j+w (AICc = 603.5; Table S8 and Fig. S4 of the Supplementary material available on Dryad). But, in light of recent criticism (Ree and Sanmartín 2018), we also evaluated models without the j parameter. For M1, the best model without the j parameter was DEC +w (AICc =621, Fig. 4a) and for M0 it was DEC (Fig. S5 of the Supplementary material available on Dryad), The M1-DEC+w model for M1 matrix was therefore the model preferred for our biogeographic analysis. We inferred a broad geographical range for the ancestor of mormyrids (Fig. 4a, NS+UG+LG+CB+Z). Further, we find six independent colonization events from Congo Basin ancestors to the East Coast and seven independent colonization events from the Nilo-Sudanic to the Upper Guinea regions. For additional details on biogeographic model comparisons see Supplementary Results available on Dryad and Table S9 of the Supplementary material available on Dryad.

DISCUSSION

The new phylogeny provides a robust comparative framework that enables detailed comparative analysis of morphological transformations and biogeography while at the same time accounting for phylogenetic uncertainty. New findings discussed in supplementary results taxonomic findings on Dryad also include important taxonomic updates necessary for this group.

Phylogenomics and Classification of Osteoglossomorpha

This study provides the most robust hypothesis of osteoglossomorph relationships to date based on both rich taxon sampling (179 or ~69% of the species) and deep gene coverage (546 exons; Figs. 1–3). The phylogenetic placement of the monotypic family Pantodontidae has been contentious among previous studies based on morphological data (Fig. 1a–d) but our results confidently placed *Pantodon buchholzi* as the sister-group of all other osteoglossiforms, in agreement with other molecular hypotheses (Lavoué and Sullivan 2004; Inoue et al. 2009; Lavoué et al. 2011; Betancur-R et al. 2017; Hughes et al. 2018). Unique to our study is the unparalleled phylogenetic resolution within Mormyridae that includes 144 species (~65% of the known diversity), compared to the previous largest

phylogeny that included 41 species and was based on only two molecular markers (Levin and Golubtsov 2018). We identify for the first time a rapid mormyrid radiation that originated ~13.1 Ma (Clade C+, Figs. 3 and 4) and highlight the need for taxonomic revisions (Supplementary Results, Taxonomic Findings available on Dryad).

Biogeography of Mormyridae

The current distribution of mormyrids is inferred to be a result of multiple vicariance event resulting in range reductions from a broad ancestral range. Our results indicate that the diversification of mormyrids was influenced by hydrological changes following geological and climatological events in Africa during the past 50 million years. The Miocene was characterized by widespread uplifting giving rise to present-day features of the Congo Basin, Angola, and East African rivers (Lavier et al. 2001; Sepulchre et al. 2006). This was a time of global climate change with warm temperatures and high precipitation rates triggering a "climate optimum" from 17–15 Ma (Flower and Kennett 1994; Zachos et al. 2001) that increased river discharge and connectivity and is thought to have promoted freshwater diversification (Livingstone et al. 1982). Our findings indicate that two diverse groups, Clade C+ in the Congo and Nilo-Sudanic basins (57 species) and *Paramormyrops, Ivindomyrus*, *Boulengeromyrus*, *and Cryptomyrus* (clade "PIBC," with 58 species) in the Lower Guinea region, originated during this time (Fig. 4a). Studies of other freshwater organisms in Africa also report substantial cladogenesis during the Miocene (Day et al. 2013; Daniels et al. 2015; Arroyave et al. 2020).

The Congo Basin covers 4 million km^2 and has the highest diversity of fishes in Africa, with ~1200 species, 80% of which are endemic (Stiassny et al. 2011). Hydrographic barriers within the Congo Basin are important at a population level in promoting diversification and preventing population mixing (Markert et al. 2010; Alter et al. 2017). However, how species-level diversity arose or is maintained in the Congo Basin is unknown (Day et al. 2017). Previous studies distinguished alternative hypotheses for African freshwater diversity, contrasting dispersal out of the Congo Basin (source) from dispersal into the Congo Basin (sink) (Livingstone et al. 1982). Fishes such as *Distichodus* and *Hydrocynus* (Characiformes), have their inferred ancestral range in the Congo Basin, supporting the source hypothesis (Goodier et al. 2011; Arroyave et al. 2020). Studies of catfishes (*Synodontis)* and spiny eels (*Mastacembelus*), on the other hand, infer multiple invasions into the Congo Basin from a much broader ancestral range (Day et al. 2013, 2017). This seems to be the case of mormyrids, given their inferred ancestral ranges that include most biogeographic regions (Fig. 4a). Our results support scenarios with multiple range reductions from this broad ancestral distribution to only the Congo Basin, suggesting that some extant taxa may have a relictual distribution in this basin indicating the Congo Basin is a sink for mormyrid diversity. It is possible that more stable conditions in the Congo basin than in other African basins after the Miocene events and throughout recent geological time provided greater opportunities for persistence. Moreover, we also show more recent speciation events in the Congo basin itself, most notably for Clade C+, *Petrocephalus*, and *Mormyrops*, after the Miocene. More studies focusing on continental distributions of African freshwater taxa are needed to understand how climate change coupled with geological and hydrological events affected their diversification.

Evolution of Craniofacial morphology in Mormyrids

Repeated origin of distinctive CFMs among mormyrids could be inferred with detail, revealing a complex pattern of evolution (Fig. 4). Our results establish that an ancestral blunt-nose condition gave rise to tubesnouts four times, such as *Mormyrops boulengeri and Mormyrops zanclirostris* and species of *Mormyrus* (Figs. 1j and 2), and the widespread chin-swelling phenotype six times—providing *prima facie* evidence for this trait's adaptive value even though very little is known about its fine structure and function. Therefore, the elongation of the snout and the origin of a fleshy extension of the lower jaw followed independent paths leading to these two characteristic CFMs. In contrast, evolution of the most extreme morphologies, the Schnauzenorgan and the tubesnout with Schnauzenorgan, seems contingent on an ancestral chin-swelling phenotype that underwent extreme elongation of the snout. The outcome of this elongation, inferred to have happen three times independently, is a tubesnout phenotype that also carries a Schnauzenorgan (*Campylomormyrus*, *Gnathonemus echidnorhynchus*, and *Genyomyrus*; Figs. 1m and 3). Direct evolution of the Schnauzenorgan (extending from the lower jaw) from a chin-swelling ancestor is not supported by our analysis and seems to depend on the concurrent elongation of the snout. Species that only carry a Schnauzenorgan (*Gnathonemus petersii and Gnathonemus longibarbis*; Figs. 1k and 3) seem mostly likely derived by the shortening of an ancestral tubesnout with Schnauzenorgan. Previous phylogenetic studies were unable to resolve some key mormyrid relationships with confidence (Sullivan et al. 2000, 2002; Lavoué et al. 2000 and the highly derived appearance of the Schnauzenorgan and the tubesnouts with Schnauzenorgan were thought to have a single origin, challenging taxonomic designations in this group. Future anatomical and developmental studies of these structures may provide critical evidence and necessary details to unravel the processes leading to these unique CFMs.

The high species diversity reported for mormyrids in the Congo Basin includes all craniofacial phenotypes with elongated snouts (tubesnouts), species with a Schnauzenorgan, and the combination of tubesnout with Schnauzenorgan. Most of the transformations to these unique CFMs originated in the Congo, or across

a wider area that includes the Congo (Fig. 4, TS1 − TS4, TS + S1 − TS + S3). Although the functional morphology of these CFMs is poorly known, tubesnouts are densely covered in electroreceptors (Castelló et al. 2000; Hollmann et al. 2008), and they may play an important role for locating prey in rocky substrates with poor visibility, especially for nocturnal species. A recent study of *Campylomormyrus* (species harboring tubesnout with Schnauzenorgan) reported associations between habitat type (sandy bottom or rocky substrate) and length of the tubesnout (Amen et al. 2020). Longer tubesnouts were found more often in rocky habitats, suggesting that this phenotype may allow them to penetrate further into the substrate to search for prey. The diversity of habitats in the Congo includes reef-like rocky bottoms filled with interstices caused by fast-flowing rapids, especially in the lower basin. Ecological studies characterizing niche partitioning among mormyrids in this highly variable river could be combined with our new phylogenetic results to better understand the origin, distribution, and maintenance of their unique CFMs.

Comparative studies reveal interesting convergences between mormyrids and Neotropical Gymnotiformes, another group of electric fishes that evolved the tubesnout phenotype multiple times (Castelló et al. 2000; Albert 2001; Hollmann et al. 2008; Evans et al. 2017) and similar foraging modalities (Marrero and Winemiller 1993). Gymnotiforms capture prey using their pincer-like jaws to extract them from the substrate and then suck them into their mouth through the tubesnout. These striking similarities in structure, function, and behavior between mormyrids and gymnotiforms may be a secondary consequence of their independent evolution of electric signaling to navigate and locate their prey (Lavoué et al. 2012). More generally, the tubesnout phenotype appears to have evolved more times in marine fishes than in freshwater fishes. Besides gymnotiforms and mormyrids, the armored stickleback (*Indostomus*, Anabantaria), and a few species of freshwater pipefishes (*Enneacampus*, *Doryichthys*, and *Microphis*; Syngnatharia) also evolved this phenotype. In contrast, several marine taxa with tubesnouts are known especially from coral reefs, including many butterflyfish species (Chaetodontidae), wrasses (*Gomphosus* and *Siphognathus*; Labridae), spikefishes (Triacanthodidae), the tubesnout (*Aulorhynchus*; Perciformes), and many taxa within Syngnatharia (snipefish, *Marcroramphosus*; seamoths, Pegasidae; seahorses and pipefishes, Syngnathidae; trumpetfishes, Aulostomidae; and cornetfish, Fistulariidae). Unlike electric gymnotiforms and mormyrids, these fishes are visual predators and use either suction feeding or grasp feeding, suggesting that the interaction of feeding mode with electrolocation may provide opportunities for the evolution of novel phenotypes.

Tempo of Osteoglossomorph Diversification

The ages of divergence estimated for the major clades are relatively older in our study compared to those obtained by Lavoué (2016) and others (Table S2 of the Supplementary material available on Dryad). Our analysis was informed by a recent reexamination of the paleontological record, summarized by Hilton and Lavoué (2018), that justified the exclusion of several fossil taxa from our analyses (†*Joffrichthys*, †*Ostariostoma*, †*Singida*, †*Chauliopareion*) that were previously used for calibration (Lavoué 2016). Even though osteoglossomorphs are well known for their abundant fossil record, uncertainty of fossil ages and affinities may lead to significant differences in estimates of divergence times. For example, a recent study excluding the contentious fossil †*Chanopsis* changed the estimated age of origin for Osteoglossidae from 124 Ma to 82.8 Ma (Capobianco and Friedman 2019). By conservatively excluding †*Chanopsis* from our analysis, we estimated the age of Osteoglossidae to 87.2 Ma (90.8–82.2 Ma, Table S5 of the Supplementary material available on Dryad). The age of Osteoglossomorpha remains contentious with a recent study placing the oldest fossils around 182.4 Ma (range 206.9–167 Ma, Capobianco and Friedman (2019)), significantly younger than most molecular estimates including the present study (235.8–223 Ma, mean 227.4 Ma; Table S5 of the Supplementary material available on Dryad). Although the incompleteness of the fossil record may partially account for this ghost lineage, finding stem osteoglossomorph fossils older than 207 Ma may be very unlikely (Capobianco and Friedman 2019). In their review of the fossil evidence, these authors noted that fossil-based estimates relied on the temporal distribution of nonmarine deposits. Since a significant part of the early evolutionary history of teleosts has likely transpired in marine environments (Betancur-R et al. 2015; Sallan et al. 2018), future discovery and inclusion of marine fossils may help to resolve the molecular-fossil gap in estimates of divergence times.

The disjunct distribution of extant osteoglossomorphs on different continents can be reexamined considering our estimated divergence times. Contrasting hypotheses include vicariance due to the breakup of the supercontinent of Gondwana (Nelson 1969; Cracraft 1974; Lundberg 1993; Li et al. 1997; Cavin 2008; Inoue et al. 2009) and marine ancestry with transoceanic dispersal followed by multiple invasions to freshwater habitats (Taverne 1998; Bonde 2008; Forey and Hilton 2015). We find that distributions of both *Arapaima* (South America) and *Heterotis* (Africa) (45.4 Ma, HPD 48.2–41.6 Ma) and Asian and African notopterids (69.29 Ma, HPD 78.7–60.3 Ma) are too young to be explained by vicariance associated with continental breakup, as South America and Africa split ~110 Ma and India and Madagascar diverged from Africa ~140 Ma, in agreement with the results of Lavoué (2016). Additionally, the divergence of *Scleropages* (SEA/Australia) and *Osteoglossum* (South America) dated at 38.2 Ma (HPD 50.9–24.9 Ma) also suggests marine dispersal (but see Supplementary material available on Dryad for an alternative calibration).

Conclusions

The radiation of the ancient clade of bony-tongue fishes in the Late Triassic gave rise to unique forms among teleosts that are currently distributed in freshwater habitats throughout the world. Rather than vicariant events due to continental drift, this pattern is best explained by hypotheses that involve widespread marine ancestors that are now extinct and multiple marine-to-freshwater transitions punctuating their long existence. The diversity of bonytongues in African freshwater habitats is predominantly due to a single family (Mormyridae) that evolved electric organs and the capacity to use electroreception as a major evolutionary innovation. This family also includes extreme anatomical phenotypes (chin-swelling, Schnauzenorgan, tubesnouts with Schnauzenorgan, and tubesnouts) comprising craniofacial structures not seen in any other group of fishes. Multiple instances of convergent evolution documented here for these CFMs make mormyrids an interesting study system to understand underlying developmental and ecological constraints. Biogeographic analysis of mormyrids reveals that this diversity is highly concentrated in the Congo Basin, suggesting that niche partitioning and electrosensory adaptations may have played a major role in this basin, possibly due to the high heterogeneity and complexity of its environments, especially in the lower Congo basin. Taxon-rich phylogenomic studies provide a robust basis for describing and explaining the diversification of ancient groups such as Osteoglossomorpha.

Supplementary Material

Data available from the Dryad Digital Repository: http://dx.doi.org/10.5061/dryad.31zcrjdkm.

Funding

This project was funded by the National Science Foundation (NSF) [DEB-1932759 and DEB-1929248 to R.B., DEB-2015404 to D.A., DEB-1457426 and DEB-1541554 to G.O.]. Additionally, the Harlan Endowment to the George Washington University provided R.D.P. with summer funding. Finally, we would like to thank Iridian Genomes Inc. for providing funding to R.D.P. for short-read genome sequencing.

Acknowledgments

We thank the following colleagues for providing samples: C.B.D. and Charles Dardia (CUMV) and for hosting R.D.P. during her time at CUMV's collection, Melanie Stiassny and Thomas R. Vigliotta (AMNH) and for hosting R.D.P., J.P.S., and C.D.H. during their stay at the AMNH's collection, Roger Bills (SAIAB), Johnathan Armbruster and David Werneke (AUMNH), Larry Page and Robert Robins (FLMNH), Andrew Simons (BMUM), Donald. J. Stewart (SUNY College of Environmental Science and Forestry), J.P.S., Diane Pitassy, and Carole Baldwin (USNM) and Leo Smith and Andy Bentley (KU). The Laboratory of Analytical Biology at NMNH LAB for providing space to conduct DNA extractions. Thanks to the Pegasus HPC and Colonial One HPC clusters (the George Washington University) personnel for providing support for data processing and phylogenetic analyses. Three anonymous reviewers provided insightful comments to improve the manuscript.

References

Albert J.S. 2001. Species diversity and phylogenetic systematics of american knifefishes (Gymnotiformes, Teleostei). Misc. Publ. Mus. Zool. Univ. Michigan. 1–140.

Alter S.E., Munshi-South J., Stiassny M.L.J. 2017. Genomewide SNP data reveal cryptic phylogeographic structure and microallopatric divergence in a rapids-adapted clade of cichlids from the Congo River. Mol. Ecol. 26:1401–1419.

Amen R., Nagel R., Hedt M., Kirschbaum F., Tiedemann R. 2020. Morphological differentiation in African weakly electric fish (genus *Campylomormyrus*) relates to substrate preferences. Evol. Ecol. 34:427–437.

Amey-Özel M., Hollmann M., von der Emde G. 2012. From the Schnauzenorgan to the back: morphological comparison of mormyromast electroreceptor organs at different skin regions of Gnathonemus petersii. J. Morphol. 273:629–638.

Arratia G. 1999. The monophyly of Teleostei and stem-group teleosts. Consensus and disagreements. Mesozoic fishes 2 — systematics and fossil. Verlag Dr. F. Pfeil. p. 265–334.

Arroyave J., Denton J.S.S., Stiassny M.L.J. 2020. Pattern and timing of diversification in the African freshwater fish genus *Distichodus* (Characiformes: Distichodontidae). BMC Evol. Biol. 20:48.

Bacelo J., Engelmann J., Hollmann M., Von Der Emde G., Grant K. 2008. Functional foveae in an electrosensory system. J. Comp. Neurol. 511:342–359.

Benton M.J., Donoghue P.C.J., Asher R.J., Friedman M., Near T.J., Vinther J. 2015. Constraints on the timescale of animal evolutionary history. Palaeontol. Electron. 18:1–107.

Betancur-R R., Ortí G., Pyron R.A. 2015. Fossil-based comparative analyses reveal ancient marine ancestry erased by extinction in ray-finned fishes. Ecol. Lett. 18:441–450.

Betancur-R R., Wiley E.O., Arratia G., Acero A., Bailly N., Miya M., Lecointre G., Ortí G. 2017. Phylogenetic classification of bony fishes. BMC Evol. Biol. 17:162.

Bolger A.M., Lohse M., Usadel B. 2014. Trimmomatic: a flexible trimmer for Illumina sequence data. Bioinformatics 30:2114–2120.

Bollback J.P. 2006. SIMMAP: stochastic character mapping of discrete traits on phylogenies. BMC Bioinformatics 7:1–7.

Bonde N. 2008. Osteoglossomorphs of the marine Lower Eocene of Denmark – with remarks on other Eocene taxa and their importance for palaeobiogeography. Geol. Soc. London, Spec. Publ. 295:253–310.

Broughton R.E., Betancur-R R., Li C., Arratia G., Ortí G. 2013. Multi-locus phylogenetic analysis reveals the pattern and tempo of bony fish evolution. PLoS Curr. 5:ecurrents.tol.2ca8041495ffafd0c92756e75247483e.

Capobianco A., Friedman M. 2019. Vicariance and dispersal in southern hemisphere freshwater fish clades: a palaeontological perspective. Biol. Rev. 94:662–699.

Caputi A.A., Carlson B.A., Macadar O. 2005. Electric organs and their control BT - electroreception. In: Bullock T.H., Hopkins C.D., Popper A.N., Fay R.R., editors. New York, NY: Springer. p. 410–451.

Castelló M.E., Aguilera P.A., Trujillo-cenóz O., Caputi A.A. 2000. Electroreception in *Gymnotus carapo*: pre-receptor processing and the distribution of electroreceptor types. 3287:3279–3287.

Cavin L. 2008. Palaeobiogeography of Cretaceous bony fishes (Actinistia, Dipnoi and Actinopterygii). Geol. Soc. Spec. Publ. 295:165–183.

Cracraft J. 1974. Continental drift and vertebrate distribution. Annu. Rev. Ecol. Syst. 5:215–261.
Crampton W.G.R. 1998. Electric signal design and habitat preferences in a species rich assemblage of gymnotiform fishes from the Upper Amazon Basin. An. Acad. Bras. Cienc. 70:805–847.
Daniels S.R., Phiri E.E., Klaus S., Albrecht C., Cumberlidge N. 2015. Multilocus phylogeny of the afrotropical freshwater crab fauna reveals historical drainage connectivity and transoceanic dispersal since the Eocene. Syst. Biol. 64:549–567.
Day J.J., Fages A., Brown K.J., Vreven E.J., Stiassny M.L.J., Bills R., Friel J.P., Rüber L. 2017. Multiple independent colonizations into the Congo Basin during the continental radiation of African *Mastacembelus* spiny eels. J. Biogeogr. 44:2308–2318.
Day J.J., Peart C.R., Brown K.J., Friel J.P., Bills R., Moritz T. 2013. Continental diversification of an African catfish radiation (Mochokidae: *Synodontis*). Syst. Biol. 62:351–365.
de Souza J.E.S., Lopes K.D.P., Teixeira D.G., Furtado C., Sakamoto T., Hamoy I.G., Lima J.P.M.S. 2018. Whole genome sequencing of the Pirarucu (*Arapaima gigas*) supports independent emergence of major teleost clades. Genome Biol. Evol. 10:2366–2379.
Dupin J., Matzke N.J., Särkinen T., Knapp S., Olmstead R.G., Bohs L., Smith S.D. 2017. Bayesian estimation of the global biogeographical history of the Solanaceae. J. Biogeogr. 44:887–899.
Evans K.M., Waltz B., Tagliacollo V., Chakrabarty P., Albert J.S. 2017. Why the short face? Developmental disintegration of the neurocranium drives convergent evolution in neotropical electric fishes. Ecol. Evol. 7:1783–1801.
Flower B.P., Kennett J.P. 1994. The middle Miocene climatic transition: East Antarctic ice sheet development, deep ocean circulation and global carbon cycling. Palaeogeogr. Palaeoclimatol. Palaeoecol. 108:537–555.
Forey, Peter L. and Hilton E.J. 2015. Two new tertiary osteoglossid fishes (Teleostei: Osteoglossomorpha) with notes on the history of the family. Herpetol. Rev. 46:1.
Gallant J.R., Losilla M., Tomlinson C., Warren W.C. 2017. The genome and adult somatic transcriptome of the mormyrid electric fish *Paramormyrops kingsleyae*. Genome Biol. Evol. 9:3525–3530.
Gallant J.R., Traeger L.L., Volkening J.D., Moffett H., Chen P.H., Novina C.D., Phillips G.N., Anand R., Wells G.B., Pinch M., Güth R., Unguez G.A., Albert J.S., Zakon H.H., Samanta M.P., Sussman M.R. 2014. Genomic basis for the convergent evolution of electric organs. Science (80-). 344:1522–1525.
Giles S., Xu G.H., Near T.J., Friedman M. 2017. Early members of "living fossil" lineage imply later origin of modern ray-finned fishes. Nature 549:265–268.
Goodier S.A.M., Cotterill F.P.D., O'Ryan C., Skelton P.H., de Wit M.J. 2011. Cryptic Diversity of African Tigerfish (Genus *Hydrocynus*) Reveals Palaeogeographic Signatures of Linked Neogene Geotectonic Events. PLoS One 6:e28775.
Greenwood P.H. 1972. New fish fossils from the Pliocene of Wadi Natrun, Egypt. J. Zool. 503–519.
Greenwood P.H., Rosen D.E., Weitzman S.H., Myers G.S. 1966. Phyletic studies of teleostean fishes, with a provisional classification of living forms. Bull. Am. Museum Nat. Hist. 133:339–456.
Hilton E.J. 2003. Comparative osteology and phylogenetic systematics of fossil and living bony-tongue fishes (Actinopterygii, Teleostei, Osteoglossomorpha). Zool. J. Linn. Soc. 137:1–100.
Hilton E.J., Grande L. 2008. Fossil Mooneyes (Teleostei: Hiodontiformes, Hiodontidae) from the Eocene of western North America, with a reassessment of their taxonomy. Geol. Soc. Spec. Publ. 295:221–251.
Hilton E.J., Lavoué S. 2018. A review of the systematic biology of fossil and living bony-tongue fishes, Osteoglossomorpha (Actinopterygii: Teleostei). Neotrop. Ichthyol. 16:1–35.
Hoang D.T., Chernomor O., von Haeseler A., Minh B.Q., Vinh L.S. 2018. UFBoot2: improving the ultrafast bootstrap approximation. Mol. Biol. Evol. 35:518–522.
Hollmann M., Engelmann J., Von Der Emde G. 2008. Distribution, density and morphology of electroreceptor organs in mormyrid weakly electric fish: Anatomical investigations of a receptor mosaic. J. Zool. 276:149–158.
Hopkins C.D., Bass A.H. 1981. Temporal coding of species recognition signals in an electric fish. Science (80-). 212:85–87.
Hughes L.C., Ortí G., Huang Y., Sun Y., Baldwin C.C., Thompson A.W., Arcila D., Betancur-R. R., Li C., Becker L., Bellora N., Zhao X., Li X., Wang M., Fang C., Xie B., Zhou Z., Huang H., Chen S., Venkatesh B., Shi Q. 2018. Comprehensive phylogeny of ray-finned fishes (Actinopterygii) based on transcriptomic and genomic data. Proc. Natl. Acad. Sci. 115:6249–6254.
Hughes L.C., Ortí G., Saad H., Li C., White W.T., Baldwin C.C., Crandall K.A., Arcila D., Betancur-R R. 2021. Exon probe sets and bioinformatics pipelines for all levels of fish phylogenomics. Mol. Ecol. Resour. 21:816–833.
Inoue J.G., Kumazawa Y., Miya M., Nishida M. 2009. The historical biogeography of the freshwater knifefishes using mitogenomic approaches: a Mesozoic origin of the Asian notopterids (Actinopterygii: Osteoglossomorpha). Mol. Phylogenet. Evol. 51:486–499.
Kalyaanamoorthy S., Minh B.Q., Wong T.K.F., Von Haeseler A., Jermiin L.S. 2017. ModelFinder: fast model selection for accurate phylogenetic estimates. Nat. Methods. 14:587–589.
Kawasaki M. 2005. Physiology of tuberous electrosensory systems. In: Bullock T.H., Hopkins C.D., Popper A.N., Fay R.R., editors. Electroreception. New York: Springer. p. 154–194.
Lamanna F., Kirschbaum F., Waurick I., Dieterich C., Tiedemann R. 2015. Cross-tissue and cross-species analysis of gene expression in skeletal muscle and electric organ of African weakly-electric fish (Teleostei; Mormyridae). BMC Genomics. 16:1–17.
Landis M.J., Matzke N.J., Moore B.R., Huelsenbeck J.P. 2013. Bayesian analysis of biogeography when the number of areas is large. Syst. Biol. 62:789–804.
Lavier L.L., Steckler M.S., Brigaud F. 2001. Climatic and tectonic control on the Cenozoic evolution of the West African margin. Mar. Geol. 178:63–80.
Lavoué S. 2016. Was Gondwanan breakup the cause of the intercontinental distribution of Osteoglossiformes? A time-calibrated phylogenetic test combining molecular, morphological, and paleontological evidence. Mol. Phylogenet. Evol. 99:34–43.
Lavoué S., Bigorne R., Lecointre G., Agnèse J.F. 2000. Phylogenetic relationships of mormyrid electric fishes (Mormyridae; Teleostei) inferred from cytochrome b sequences. Mol. Phylogenet. Evol. 14:1–10.
Lavoué S., Miya M., Arnegard M.E., McIntyre P.B., Mamonekene V., Nishida M. 2011. Remarkable morphological stasis in an extant vertebrate despite tens of millions of years of divergence. Proc. R. Soc. B Biol. Sci. 278:1003–1008.
Lavoué S., Miya M., Arnegard M.E., Sullivan J.P., Hopkins C.D., Nishida M. 2012. Comparable ages for the independent origins of electrogenesis in African and South American weakly electric fishes. PLoS One 7:1–18.
Lavoué S., Sullivan J.P. 2004. Simultaneous analysis of five molecular markers provides a well-supported phylogenetic hypothesis for the living bony-tongue fishes (Osteoglossomorpha: Teleostei). Mol. Phylogenet. Evol. 33:171–185.
Lévêque C., Oberdorff T., Paugy D., Stiassny M.L.J., Tedesco P.A. 2008. Global diversity of fish (Pisces) in freshwater. Hydrobiologia 595:545–567.
Levin B.A., Golubtsov A.S. 2018. New insights into the molecular phylogeny and taxonomy of mormyrids (Osteoglossiformes, Actinopterygii) in northern East Africa. J. Zool. Syst. Evol. Res. 56:61–76.
Li G.-Q., Wilson M.V.H. 1996. Phylogeny of Osteoglossomorpha. In: Stiassny M.L.J., Parenti L.R., Johnson G.D., editors. Interrelationships of fishes. New York: Academic Press. p. 163-174.
Li G.-Q., Wilson M.V.H., Grande L. 1997. Review of †Eohiodon (Teleostei: Osteoglossomorpha) from western North America, with a phylogenetic reassessment of Hiodontidae. J. Paleontol. 71:1109–1124.
Li G.-Q., Wilsoni M.V.H. 1996. The discovery of †Heterotidinae (teleostei: Osteoglossidae) from the paleocene paskapoo formation of Alberta, Canada. J. Vertebr. Paleontol. 16:198–209.
Lissmann H.W. 1958. On the function and evolution of electric organs in fish. J. Exp. Biol. 35:156-.
Livingstone D.A., Rowland M., Bailey P.E. 1982. On the size of African riverine fish faunas. Integr. Comp. Biol. 22:361–369.

Lundberg J.G. 1993. African-South American freshwater fish clades and continental drift: problems with a paradigm. Biol. relationships between Africa South Am. 156–199.

Luo R., Liu B., Xie Y., Li Z., Huang W., Yuan J., He G., Chen Y., Pan Q., Liu Y., Tang J., Wu G., Zhang H., Shi Y., Liu Y., Yu C., Wang B., Lu Y., Han C., Cheung D.W., Yiu S.M., Peng S., Xiaoqian Z., Liu G., Liao X., Li Y., Yang H., Wang J., Lam T.W., Wang J. 2015. Erratum to "SOAPdenovo2: An empirically improved memory-efficient short-read de novo assembler" [GigaScience, (2012), 1, 18]. Gigascience 4:1.

Mai U., Mirarab S. 2018. TreeShrink: fast and accurate detection of outlier long branches in collections of phylogenetic trees. BMC Genomics. 19:272.

Markert J.A., Schelly R.C., Stiassny M.L. 2010. Genetic isolation and morphological divergence mediated by high-energy rapids in two cichlid genera from the lower Congo rapids. BMC Evol. Biol. 10:149.

Marrero C., Winemiller K.O. 1993. Tube-snouted gymnotiform and mormyriform fishes: convergence of a specialized foraging mode in teleosts. Environ. Biol. Fishes. 38:299–309.

Matzke N.J. 2013. BioGeoBEARS: BioGeography with Bayesian (and likelihood) evolutionary analysis in R Scripts. R Packag. version 0.2. 1:2013.

Matzke N.J. 2014. Model selection in historical biogeography reveals that founder-event speciation is a crucial process in island clades. Syst. Biol. 63:951–970.

Montoya-Burgos J.I. 2003. Historical biogeography of the catfish genus *Hypostomus* (Siluriformes: Loricariidae), with implications on the diversification of Neotropical ichthyofauna. Mol. Ecol. 12:1855–1867.

Murray A.M., Zelenitsky D.K., Brinkman D.B., Neuman A.G. 2018. Two new Palaeocene osteoglossomorphs from Canada, with a reassessment of the relationships of the genus †*Joffrichthys*, and analysis of diversity from articulated versus microfossil material. Zool. J. Linn. Soc. 183:907–944.

Nelson G.J. 1969. Infraorbital bones and their bearing on the phylogeny and geography of osteoglossomorph fishes. Am. Mus. Nov. 2394:1–37.

Nguyen L.T., Schmidt H.A., Von Haeseler A., Minh B.Q. 2015. IQ-TREE: a fast and effective stochastic algorithm for estimating maximum-likelihood phylogenies. Mol. Biol. Evol. 32:268–274.

Ranwez V., Douzery E.J.P., Cambon C., Chantret N., Delsuc F. 2018. MACSE v2: Toolkit for the alignment of coding sequences accounting for frameshifts and stop codons. Mol. Biol. Evol. 35:2582–2584.

Ree R.H., Sanmartín I. 2018. Conceptual and statistical problems with the DEC+J model of founder-event speciation and its comparison with DEC via model selection. J. Biogeogr. 45:741–749.

Ree R.H., Smith S.A. 2008. Maximum likelihood inference of geographic range evolution by dispersal, local extinction, and cladogenesis. Syst. Biol. 57:4–14.

dos Reis M., Yang Z. 2019. Bayesian molecular clock dating using genome-scale datasets BT - evolutionary genomics: statistical and computational methods. In: Anisimova M., editor. New York, NY: Springer New York. p. 309–330.

Revell L.J. 2012. phytools: an R package for phylogenetic comparative biology (and other things). Methods Ecol. Evol. 3:217–223.

Rincon-Sandoval M., Duarte-Ribeiro E., Davis A.M., Santaquiteria A., Hughes L.C., Baldwin C.C., Soto-Torres L., Acero P. A., Walker H.J., Carpenter K.E., Sheaves M., Ortí G., Arcila D., Betancur-R. R. 2020. Evolutionary determinism and convergence associated with water-column transitions in marine fishes. Proc. Natl. Acad. Sci. 117:33396–33403.

Ronquist F. 1997. Dispersal-vicariance analysis: a new approach to the quantification of historical biogeography. Syst. Biol. 46: 195–203.

Sallan L., Friedman M., Sansom R.S., Bird C.M., Sansom I.J. 2018. The nearshore cradle of early vertebrate diversification. Science (80-) 362:460–464.

Santaquiteria A., Siqueira A.C., Duarte-Ribeiro E., Carnevale G., White W., Pogonoski J., Baldwin C.C., Ortí G., Arcila D., Betancur-R. R. 2021. Phylogenomics and historical biogeography of seahorses, dragonets, goatfishes, and allies (Teleostei: Syngnatharia): assessing the factors driving uncertainty in biogeographic inferences. Syst. Biol.

Sayyari E., Mirarab S. 2016. Fast coalescent-based computation of local branch support from quartet frequencies. Mol. Biol. Evol. 33:1654–1668.

Sepulchre P., Ramstein G., Fluteau F., Schuster M., Tiercelin J.J., Brunet M. 2006. Tectonic uplift and Eastern Africa aridification. Science (80-) 313:1419–1423.

Simmons M.P., Gatesy J. 2021. Collapsing dubiously resolved gene-tree branches in phylogenomic coalescent analyses. Mol. Phylogenet. Evol. 158:107092.

Steindachner F. 1866. Ichthyologische Mittheilungen. (IX.). Verhandlungen der K.-K. Zool. Gesellschaft Wien. 16:761–796, Pls. 13-18.

Stendall W. 1916. Die schnauzenorgane der mormyriden. Zeit wiss Zool. 115:650–670.

Stiassny M.L.J., Brummett R.E., Harrison I.J., Monsembula R., Mamonekene V. 2011. The status and distribution of freshwater fishes in central Africa. status Distrib. Freshw. Biodivers. Cent. Africa 27–46.

Sullivan J.P., Lavoué S., Hopkins C.D. 2000. Molecular systematics of the African electric fishes (Mormyroidea: teleostei) and a model for the evolution of their electric organs. J. Exp. Biol. 203:665–683.

Sullivan J.P., Lavoué S., Hopkins C.D. 2002. Discovery and phylogenetic analysis of a riverine species flock of African electric fishes (Mormyridae: Teleostei). Evolution (NY) 56:597–616.

Taverne L. 1998. Les ostéoglossomorphes marins de l'Éocène du Monte Bolca (Italie): Monopteros Volta 1796, Thrissopterus Heckel, 1856 et Foreyichthys Taverne, 1979. Considérations sur la phylogénie des téléostéens ostéoglossomorphes. Stud. e Ric. sui Giacimenti Terziari di Bolca. 7:67–158.

Wheeler T.J., Eddy S.R. 2013. Nhmmer: DNA homology search with profile HMMs. Bioinformatics 29:2487–2489.

Wilson M.V.H., Murray A.M. 2008. Osteoglossomorpha: phylogeny, biogeography, and fossil record and the significance of key African and Chinese fossil taxa. Geol. Soc. Spec. Publ. 295:185–219.

Yang Z. 2007. PAML 4: phylogenetic analysis by maximum likelihood. Mol. Biol. Evol. 24:1586–1591.

Zachos J., Pagani H., Sloan L., Thomas E., Billups K. 2001. Trends, rhythms, and aberrations in global climate 65 Ma to present. Science (80-) 292:686–693.

Zhang C., Sayyari E., Mirarab S. 2017. ASTRAL-III: increased scalability and impacts of contracting low support branches. In: Meidanis J., Nakhleh L., editors. Comparative genomics: 15th International Workshop, RECOMB CG 2017, Barcelona, Spain, October 4–6, 2017, Proceedings. Cham: Springer International Publishing. p. 53–75.

Zhang J.-Y. 2006. Phylogeny of osteoglossomorpha. Vertebr. Palasiat. 01:43–59.